IOP Publishing New J. Phys. 27 (2025) 124504 https://doi.org/10.1088/1367-2630/ae2357

New Journal of Physics
The open access journal at the forefront of physics

Deutsche Physikalische Gesellschaft DPG
IOP Institute of Physics

Published in partnership with: Deutsche Physikalische Gesellschaft and the Institute of Physics

PAPER

Unambiguous arbitrary high-dimensional Bell states analyzer via indefinite causal order

Jun-Hai Zhao[1], Wen-Qiang Liu[2] and Hai-Rui Wei[1,*]

[1] School of Mathematics and Physics, University of Science and Technology Beijing, Beijing 100083, People's Republic of China
[2] Department of Mathematics and Physics, Shijiazhuang Tiedao University, Shijiazhuang 050043, People's Republic of China
* Author to whom any correspondence should be addressed.

E-mail: hrwei@ustb.edu.cn

Keywords: high-dimensional quantum system, indefinite causal order, quantum switch, Bell-state analyzer

OPEN ACCESS

RECEIVED
24 September 2025

REVISED
17 November 2025

ACCEPTED FOR PUBLICATION
24 November 2025

PUBLISHED
4 December 2025

Abstract

High-dimensional quantum systems greatly outperform their two-dimensional counterparts in channel capacity, quantum complexity and efficiency, quantum communication security, etc. Bell-state analyzer (BSA) is a crucial prerequisite for a number of quantum communication protocols. We propose an approach for completely and deterministically distinguishing a set of arbitrary d-dimensional ($d \geqslant 3$) Bell states via indefinite causal order (ICO). In previous schemes, bit and phase information are discriminated in succession. Exploiting the gravitational ICO as the sole resource, we propose some high-dimensional BSA schemes. Independent of the dimensions, a set of generalized Bell states are completely and deterministically discriminated by adjusting the form of the embedded local single-qudit gates within ICO switch and measuring each qudit in the $\{|0\rangle, |1\rangle, \cdots, |d-1\rangle\}$ basis. Notably, in our high-dimensional BSA process, the indefinite causal structure is not consumed. Hence a completely nondestructive high-dimensional BSA can be achieved by iterating the indefinite causal structure process for two rounds.

1. Introduction

Quantum entanglement is essential for many quantum information processing (QIP) tasks, such as quantum key distribution [1, 2], quantum dense coding [3, 4], quantum teleportation [5, 6], quantum secret sharing [7, 8], quantum entanglement swapping [9, 10], and quantum secure direct communication. An essential step in these protocols is the Bell-state analyzer (BSA) [11, 12], which is defined as an approach to distinguish all four of the Bell states. Complete and deterministic BSA is a significant prerequisite for many quantum communication tasks. Nowadays, BSA protocols have been proposed in a number of two-dimensional physical systems [13–15].

Implementing a complete and deterministic BSA still faces fundamental challenges when restricted to local operations and classical communication (LOCC). The LOCC-based protocols can perfectly discriminate any two orthogonal multipartite pure states [16, 17]. Unfortunately, this LOCC-based perfect discriminating capability is fundamentally limited when focused on a set of three (or more) entangled states. The presence of entanglement poses the key obstacle, and research confirms that the number of locally distinguishable states is constrained by the total dimension of the system over the average entanglement of the state [18, 19].

BSA was first proposed by Kwiat and Weinfurter [11] in 1998, and it relies only on linear optical elements. Subsequently, tremendous progress has been made both in theory and experiment. Polarization BSA has been experimentally demonstrated using local linear optics [13, 20, 21], and the optimal efficiency of these approaches is 50%. One strategy adopted to overcome this inherent probabilistic nature is to employ 'buses', ranging from atoms [14], cross-Kerr media [22], and artificial atoms [23] to superimpose different operations [24]. The second strategy is to introduce additional hyper-entangled Bell pairs [25]. The third strategy is to exploit additional degrees of freedom [26, 27], utilize conditioned

detection [28], or enlarge the Hilbert space [29]. The existing BSAs are mainly focused on 2-dimensional systems, while their high-dimensional scenarios remain largely unexplored.

In traditional QIP models, quantum operations are applied in a fixed sequential order. However, quantum mechanics also permits the scenarios in which two or more events take place in an indefinite order [30]. This 'superimpose different operations' is called indefinite causal order (ICO), and such quantum-controlled order of events has been experimentally confirmed [31–34]. It has been demonstrated that ICO can offer notable operational advantages over their classical fixed scenarios in various specific QIP tasks, including quantum channel discrimination [35], promise problems [36], communication complexity tasks [37, 38], quantum communication [39], quantum metrology [40, 41], quantum thermodynamics [42, 43], quantum algorithms [44], noise mitigation [45], quantum key distribution [46], and entanglement generation [47] and distillation [48].

In this work, we propose a more elegant complete and deterministic BSA in an arbitrary high-dimensional system. Exploiting ICO as the sole resource, we first propose an unambiguous BSA scheme in 3-dimensional quantum system. Then, we extend our ICO-based approach to a 4-dimensional scenario and further extend it to arbitrary d-dimensional scenarios. Subsequently, by leveraging the quantum superposition of different space-time geometries, we design a set of high-dimensional ICO gravitational switches to perfectly distinguish the corresponding set of high-dimensional generalized Bell states.

The scheme we designed for the high-dimensional BSA has the following characteristics. First, single-partite unitary operations are essential for our protocol. A perfect high-dimensional BSA is completed by adjusting the forms of the single-partite operations. Therefore, our scheme bypasses the need for nonlocal operations, material platforms, or additional entangled pairs, which are necessary for existing BSA protocols. Second, only local shift gates involved in the ICO switch are introduced, and these simple single-qudit gates are experimentally feasible. Third, non-destructive high-dimensional BSA can be achieved by iterating the ICO switch for two rounds, as the ICO is not consumed. Fourth, after one switch process and a projection measurement of the Bell state, the high-dimensional Bell states can be completely distinguished. In previous two-step schemes, bit and phase information are distinguished in succession.

The organization of this paper is as follows. In section 2, we first present the limitations of high-dimensional BSA within LOCC framework. Subsequently, we propose a scheme to completely distinguish the nine qutrit Bell states via ICO quantum 3-switch. Finally, we generalize our method to arbitrary 4-dimensional and further to arbitrary d-dimensional scenarios. In section 3, we first propose an architecture to implement space-time ICO quantum 3-switch, where the space-time ICO arises from the spatial superposition of a massive gravitating body. Subsequently, we extend our approach to the gravitational ICO quantum 4-switch and further to gravitational ICO quantum d-switch scenarios. We provide a discussion and summarize our results in section 4.

2. Complete and deterministic BSA in d-dimensional system via ICO

2.1. The limitation of the traditional LOCC-based BSA

We consider the two agents Alice and Bob who share a bipartite quantum system. Each spatially separated party can locally perform quantum operations on their own subsystem and communicates their respective classical information with each other. This LOCC is denoted by $\mathcal{O}_{\mathrm{L}}$. Obviously, set $\mathcal{O}_{\mathrm{L}}$ forms a strict subset of the set of all quantum operations (denoted by $\mathcal{O}$) performed on the arbitrary bipartite quantum state, i.e. $\mathcal{O}_{\mathrm{L}} \subset \mathcal{O}$. Operations which cannot be implemented by solely using LOCC are called nonlocal operations (denoted by $\mathcal{O}_{\mathrm{NL}}$).

In bipartite d-dimensional system, there are d^2 generalized Bell states, and the aim of this paper is to distinguish this set of the orthogonal generalized Bell states completely and deterministically. It is known that it is impossible to perfectly distinguish all d^2 generalized Bell states by using only standard LOCC. Early in 2006, Hayashi *et al* [18] provided a strict quantitative upper bound on the number N of pure states that can be perfectly distinguished by LOCC, i.e.

$$N(\mathrm{Bi}) \leqslant d_1 d_2 / \left(\sum_i \alpha_i \right)^2 . \tag{1}$$

Here the N pure states have the same entanglement (Bi). d_1 and d_2 are the dimensions of the two subsystems, respectively. α_i is the Schmidt coefficient for each pure states contained in the set.

Substituting $d_1 = d_2 = d$ and $(\sum_i \alpha_i)^2 = d$ into equation (1), we can obtain

$$N \leqslant (d \cdot d)/d = d. \tag{2}$$

This indicates that it is impossible to distinguish more than d generalized Bell states in d-dimensional system by two spatially separated parties using standard LOCC. It is thus desirable to seek alternative efficient scheme for completely implementing high-dimensional BSA in a deterministic way. In the following, we will access perfect BSA with assistance of ICO.

2.2. Deterministic BSA in 3-dimensional system via ICO 3-switch

The ICO quantum switch $\mathcal{S}$, the simplest and most common form of ICO, applies two or more events to the target system in a temporal order coherently controlled by an additional control system [49]. Now, let us detail the ICO quantum 3-switch operation.

The ICO quantum 3-switch $\mathcal{S}^3$ serves as a universal resource to map the different orthogonal basis states $|k\rangle_c$ of the additional control system to different local qutrit (i.e. three-state or three-level quantum system) operations $U_k^3 \otimes V_k^3$ on the target system. Here the subscript , and the superscript 3 denotes the 3-dimensional system. For clarity and concise exposition of the working principles of $\mathcal{S}^3$, the control system of $\mathcal{S}^3$ is initially prepared in the superposition state $|\mathcal{F}_0\rangle^c$. Here

$$|\mathcal{F}_0\rangle^c = \frac{1}{\sqrt{3}}\left(|0\rangle^c + |1\rangle^c + |2\rangle^c\right). \tag{3}$$

The two target subsystems Alice and Bob are initially prepared in the product state, $|\Psi\rangle_A^t \otimes |\Psi\rangle_B^t \in \mathbb{C}^3 \otimes \mathbb{C}^3$. The operation of $\mathcal{S}^3$ is given by

$$\begin{aligned}
\mathcal{S}^3|\mathcal{F}_0\rangle^c|\Psi\rangle_A^t|\Psi\rangle_B^t = &\frac{1}{\sqrt{3}}\left(|0\rangle^c \otimes U_1^3|\Psi\rangle_A^t \otimes V_1^3|\Psi\rangle_B^t + |1\rangle^c \otimes U_2^3|\Psi\rangle_A^t \otimes V_2^3|\Psi\rangle_B^t\right.\\
&\left.+|2\rangle^c \otimes U_3^3|\Psi\rangle_A^t \otimes V_3^3|\Psi\rangle_B^t\right)\\
=&\frac{1}{3}|\mathcal{F}_0\rangle^c\left[\left(U_1^3 \otimes V_1^3\right) + \left(U_2^3 \otimes V_2^3\right) + \left(U_3^3 \otimes V_3^3\right)\right]|\Psi\rangle_A^t|\Psi\rangle_B^t\\
&+\frac{1}{3}|\mathcal{F}_1\rangle^c\left[\left(U_1^3 \otimes V_1^3\right) + e^{i\frac{4\pi}{3}}\left(U_2^3 \otimes V_2^3\right) + e^{i\frac{2\pi}{3}}\left(U_3^3 \otimes V_3^3\right)\right]|\Psi\rangle_A^t|\Psi\rangle_B^t\\
&+\frac{1}{3}|\mathcal{F}_2\rangle^c\left[\left(U_1^3 \otimes V_1^3\right) + e^{i\frac{2\pi}{3}}\left(U_2^3 \otimes V_2^3\right) + e^{i\frac{4\pi}{3}}\left(U_3^3 \otimes V_3^3\right)\right]|\Psi\rangle_A^t|\Psi\rangle_B^t.
\end{aligned} \tag{4}$$

where

$$|\mathcal{F}_0\rangle = \frac{1}{\sqrt{3}}\left(|0\rangle^c + |1\rangle^c + |2\rangle^c\right), \tag{5}$$

$$|\mathcal{F}_1\rangle = \frac{1}{\sqrt{3}}\left(|0\rangle^c + e^{\frac{2\pi i}{3}}|1\rangle^c + e^{\frac{4\pi i}{3}}|2\rangle^c\right), \tag{6}$$

$$|\mathcal{F}_2\rangle = \frac{1}{\sqrt{3}}\left(|0\rangle^c + e^{\frac{4\pi i}{3}}|1\rangle^c + e^{\frac{2\pi i}{3}}|2\rangle^c\right). \tag{7}$$

Based on equation (4), we can see that depending on the output states $\{|\mathcal{F}_0\rangle, |\mathcal{F}_1\rangle, |\mathcal{F}_2\rangle\}$, the output target state is an entangled state by suitable choice of local qutrit operations U_k^3 and V_k^3 $(k = 1, 2, 3)$. Hence, the ICO switch $\mathcal{S}^3$ described by equation (4) serves as a sole resource and has the potential to completely discriminate nine qutrit generalized Bell states $\{|\Psi_{i,j}\rangle\}$ with $i, j \in \{0, 1, 2\}$. Here

$$|\Psi_{0,0}\rangle_{AB} = \frac{1}{\sqrt{3}}\left(|00\rangle + |11\rangle + |22\rangle\right)_{AB}, \tag{8}$$

$$|\Psi_{0,1}\rangle_{AB} = \frac{1}{\sqrt{3}}\left(|01\rangle + |12\rangle + |20\rangle\right)_{AB}, \tag{9}$$

$$|\Psi_{0,2}\rangle_{AB} = \frac{1}{\sqrt{3}}\left(|02\rangle + |10\rangle + |21\rangle\right)_{AB}, \tag{10}$$

$$|\Psi_{1,0}\rangle_{AB} = \frac{1}{\sqrt{3}}\left(|00\rangle + e^{\frac{2\pi i}{3}}|11\rangle + e^{\frac{4\pi i}{3}}|22\rangle\right)_{AB}, \tag{11}$$

$$|\Psi_{1,1}\rangle_{AB} = \frac{1}{\sqrt{3}}\left(|01\rangle + e^{\frac{2\pi i}{3}}|12\rangle + e^{\frac{4\pi i}{3}}|20\rangle\right)_{AB}, \tag{12}$$

$$|\Psi_{1,2}\rangle_{AB} = \frac{1}{\sqrt{3}}\left(|02\rangle + e^{\frac{2\pi i}{3}}|10\rangle + e^{\frac{4\pi i}{3}}|21\rangle\right)_{AB}, \tag{13}$$

$$|\Psi_{2,0}\rangle_{AB}=\frac{1}{\sqrt{3}}\left(|00\rangle+\mathrm{e}^{\frac{4\pi\mathrm{i}}{3}}|11\rangle+\mathrm{e}^{\frac{2\pi\mathrm{i}}{3}}|22\rangle\right)_{AB}, \tag{14}$$

$$|\Psi_{2,1}\rangle_{AB}=\frac{1}{\sqrt{3}}\left(|01\rangle+\mathrm{e}^{\frac{4\pi\mathrm{i}}{3}}|12\rangle+\mathrm{e}^{\frac{2\pi\mathrm{i}}{3}}|20\rangle\right)_{AB}, \tag{15}$$

$$|\Psi_{2,2}\rangle_{AB}=\frac{1}{\sqrt{3}}\left(|02\rangle+\mathrm{e}^{\frac{4\pi\mathrm{i}}{3}}|10\rangle+\mathrm{e}^{\frac{2\pi\mathrm{i}}{3}}|21\rangle\right)_{AB}. \tag{16}$$

The embedded local operations U_k^3 and V_k^3 $(k=1,2,3)$ within $\mathcal{S}^3$ given in equation (4) are adjusted as the following exponentiation functions

$$U_1^3=\left(U_{\mathrm{shift}}^3\right)^0,\quad U_2^3=\left(U_{\mathrm{shift}}^3\right)^1,\quad U_3^3=\left(U_{\mathrm{shift}}^3\right)^2, \tag{17}$$

$$V_1^3=\left(U_{\mathrm{shift}}^3\right)^1,\quad V_2^3=\left(U_{\mathrm{shift}}^3\right)^2,\quad V_3^3=\left(U_{\mathrm{shift}}^3\right)^3. \tag{18}$$

Here

$$U_{\mathrm{shift}}^3=\begin{pmatrix}0&0&1\\1&0&0\\0&1&0\end{pmatrix}. \tag{19}$$

The exponentiation function $(U_{\mathrm{shift}}^3)^0$ is a 3×3 identity matrix, $(U_{\mathrm{shift}}^3)^2=U_{\mathrm{shift}}^3\cdot U_{\mathrm{shift}}^3$, and $(U_{\mathrm{shift}}^3)^3=U_{\mathrm{shift}}^3\cdot U_{\mathrm{shift}}^3\cdot U_{\mathrm{shift}}^3$.

Based on equations (17)–(19), we can see that the conversions of $\{|\Psi_{i,j}\rangle_{AB}\}$ induced by $\mathcal{S}^3$ are given by

$$\mathcal{S}^3|\mathcal{F}_0\rangle^c|\Psi_{0,0}\rangle_{AB}=|\mathcal{F}_0\rangle^c|\Psi_{0,1}\rangle_{AB}, \tag{20}$$

$$\mathcal{S}^3|\mathcal{F}_0\rangle^c|\Psi_{0,1}\rangle_{AB}=|\mathcal{F}_0\rangle^c|\Psi_{0,2}\rangle_{AB}, \tag{21}$$

$$\mathcal{S}^3|\mathcal{F}_0\rangle^c|\Psi_{0,2}\rangle_{AB}=|\mathcal{F}_0\rangle^c|\Psi_{0,0}\rangle_{AB}, \tag{22}$$

$$\mathcal{S}^3|\mathcal{F}_0\rangle^c|\Psi_{1,0}\rangle_{AB}=|\mathcal{F}_2\rangle^c|\Psi_{1,1}\rangle_{AB}, \tag{23}$$

$$\mathcal{S}^3|\mathcal{F}_0\rangle^c|\Psi_{1,1}\rangle_{AB}=|\mathcal{F}_2\rangle^c|\Psi_{1,2}\rangle_{AB}, \tag{24}$$

$$\mathcal{S}^3|\mathcal{F}_0\rangle^c|\Psi_{1,2}\rangle_{AB}=|\mathcal{F}_2\rangle^c|\Psi_{1,0}\rangle_{AB}, \tag{25}$$

$$\mathcal{S}^3|\mathcal{F}_0\rangle^c|\Psi_{2,0}\rangle_{AB}=|\mathcal{F}_1\rangle^c|\Psi_{2,1}\rangle_{AB}, \tag{26}$$

$$\mathcal{S}^3|\mathcal{F}_0\rangle^c|\Psi_{2,1}\rangle_{AB}=|\mathcal{F}_1\rangle^c|\Psi_{2,2}\rangle_{AB}, \tag{27}$$

$$\mathcal{S}^3|\mathcal{F}_0\rangle^c|\Psi_{2,2}\rangle_{AB}=|\mathcal{F}_1\rangle^c|\Psi_{2,0}\rangle_{AB}. \tag{28}$$

Based on equations (20)–(28), we can see that according to the information of the control system, the nine Bell states $\{|\Psi_{i,j}\rangle_{AB}\}$ can be divided into three groups: $\{|\Psi_{0,0}\rangle_{AB}, |\Psi_{0,1}\rangle_{AB}, |\Psi_{0,2}\rangle_{AB}\}$ corresponding to $|\mathcal{F}_0\rangle^c$; $\{|\Psi_{1,0}\rangle_{AB}, |\Psi_{1,1}\rangle_{AB}, |\Psi_{1,2}\rangle_{AB}\}$ corresponding to $|\mathcal{F}_2\rangle^c$; and $\{|\Psi_{2,0}\rangle_{AB}, |\Psi_{2,1}\rangle_{AB}, |\Psi_{2,2}\rangle_{AB}\}$ corresponding to $|\mathcal{F}_1\rangle^c$.

The next task is only to distinguish the different relative value in each group and it can be accomplished by the projection measurement of each agent in the basis $\{|0\rangle,|1\rangle,|2\rangle\}$, see table 1. Therefore, the nine 2-qutrit Bell states can be completely and deterministically distinguished by using the ICO quantum 3-switch $\mathcal{S}^3$.

Table 1. The correspondences between the outcome of the quantum 3-switch $\mathcal{S}^3$, qutrit information, and the state transition for discriminating nine Bell states.

Outcome of 3-switch $\mathcal{S}^3$	Qutrit information of (j_A, j_B)	Output Bell state	Input Bell state
$\|\mathcal{F}_0\rangle^c$	$j_B = (j_A+1) \bmod 3$	$\|\Psi_{0,1}\rangle_{AB}$	$\|\Psi_{0,0}\rangle_{AB}$
	$j_B = (j_A+2) \bmod 3$	$\|\Psi_{0,2}\rangle_{AB}$	$\|\Psi_{0,1}\rangle_{AB}$
	$j_B = j_A$	$\|\Psi_{0,0}\rangle_{AB}$	$\|\Psi_{0,2}\rangle_{AB}$
$\|\mathcal{F}_2\rangle^c$	$j_B = (j_A+1) \bmod 3$	$\|\Psi_{1,1}\rangle_{AB}$	$\|\Psi_{1,0}\rangle_{AB}$
	$j_B = (j_A+2) \bmod 3$	$\|\Psi_{1,2}\rangle_{AB}$	$\|\Psi_{1,1}\rangle_{AB}$
	$j_B = j_A$	$\|\Psi_{1,0}\rangle_{AB}$	$\|\Psi_{1,2}\rangle_{AB}$
$\|\mathcal{F}_1\rangle^c$	$j_B = (j_A+1) \bmod 3$	$\|\Psi_{2,1}\rangle_{AB}$	$\|\Psi_{2,0}\rangle_{AB}$
	$j_B = (j_A+2) \bmod 3$	$\|\Psi_{2,2}\rangle_{AB}$	$\|\Psi_{2,1}\rangle_{AB}$
	$j_B = j_A$	$\|\Psi_{2,0}\rangle_{AB}$	$\|\Psi_{2,2}\rangle_{AB}$

2.3. Deterministic BSA in 4-dimensional system via ICO 4-switch

The operation of the quantum ICO quantum 4-switch $\mathcal{S}^4$ is given by

$$\begin{aligned}\mathcal{S}^4|\mathcal{H}_0\rangle^c|\Psi\rangle_A^t|\Psi\rangle_B^t = \frac{1}{\sqrt{4}}\big(&|0\rangle^c \otimes U_1^4|\Psi\rangle_A^t \otimes V_1^4|\Psi\rangle_B^t + |1\rangle^c \otimes U_2^4|\Psi\rangle_A^t \otimes V_2^4|\Psi\rangle_B^t \\ &+|2\rangle^c \otimes U_3^4|\Psi\rangle_A^t \otimes V_3^4|\Psi\rangle_B^t + |3\rangle^c \otimes U_4^4|\Psi\rangle_A^t \otimes V_4^4|\Psi\rangle_B^t\big).\end{aligned} \tag{29}$$

Here and afterwards,

$$|\mathcal{H}_0\rangle^c = \frac{1}{2}\left(|0\rangle + |1\rangle + |2\rangle + |3\rangle\right), \tag{30}$$

$$|\mathcal{H}_1\rangle^c = \frac{1}{2}\left(|0\rangle + \mathrm{i}|1\rangle - |2\rangle - \mathrm{i}|3\rangle\right), \tag{31}$$

$$|\mathcal{H}_2\rangle^c = \frac{1}{2}\left(|0\rangle - |1\rangle + |2\rangle - |3\rangle\right), \tag{32}$$

$$|\mathcal{H}_3\rangle^c = \frac{1}{2}\left(|0\rangle - \mathrm{i}|1\rangle - |2\rangle + \mathrm{i}|3\rangle\right). \tag{33}$$

The local ququart (i.e. 4-level or 4-state quantum system) operations U_k^4 and V_k^4 with $k = 1,2,3,4$ given in equation (29) are set as

$$U_1^4 = \left(U_{\text{shift}}^4\right)^0, \quad U_2^4 = \left(U_{\text{shift}}^4\right)^1, \quad U_3^4 = \left(U_{\text{shift}}^4\right)^2, \quad U_4^4 = \left(U_{\text{shift}}^4\right)^3, \tag{34}$$

$$V_1^4 = \left(U_{\text{shift}}^4\right)^1, \quad V_2^4 = \left(U_{\text{shift}}^4\right)^2, \quad V_3^4 = \left(U_{\text{shift}}^4\right)^3, \quad V_4^4 = \left(U_{\text{shift}}^4\right)^4, \tag{35}$$

where

$$U_{\text{shift}}^4 = \begin{pmatrix} 0 & 0 & 0 & 1 \\ 1 & 0 & 0 & 0 \\ 0 & 1 & 0 & 0 \\ 0 & 0 & 1 & 0 \end{pmatrix}. \tag{36}$$

The sixteen generalized 2-ququart Bell states $\{|\psi_{i,j}\rangle\}$ with $i,j = 0,1,2,3$ can be expressed as

$$|\psi_{0,0}\rangle_{AB} = \frac{1}{2}\left(|00\rangle + |11\rangle + |22\rangle + |33\rangle\right)_{AB}, \tag{37}$$

$$|\psi_{0,1}\rangle_{AB} = \frac{1}{2}\left(|01\rangle + |12\rangle + |23\rangle + |30\rangle\right)_{AB}, \tag{38}$$

$$|\psi_{0,2}\rangle_{AB} = \frac{1}{2}\left(|02\rangle + |13\rangle + |20\rangle + |31\rangle\right)_{AB}, \tag{39}$$

$$|\psi_{0,3}\rangle_{AB} = \frac{1}{2}\left(|03\rangle + |10\rangle + |21\rangle + |32\rangle\right)_{AB}, \tag{40}$$

$$|\psi_{1,0}\rangle_{AB}=\frac{1}{2}\left(|00\rangle+\mathrm{i}|11\rangle-|22\rangle-\mathrm{i}|33\rangle\right)_{AB},\tag{41}$$

$$|\psi_{1,1}\rangle_{AB}=\frac{1}{2}\left(|01\rangle+\mathrm{i}|12\rangle-|23\rangle-\mathrm{i}|30\rangle\right)_{AB},\tag{42}$$

$$|\psi_{1,2}\rangle_{AB}=\frac{1}{2}\left(|02\rangle+\mathrm{i}|13\rangle-|20\rangle-\mathrm{i}|31\rangle\right)_{AB},\tag{43}$$

$$|\psi_{1,3}\rangle_{AB}=\frac{1}{2}\left(|03\rangle+\mathrm{i}|10\rangle-|21\rangle-\mathrm{i}|32\rangle\right)_{AB},\tag{44}$$

$$|\psi_{2,0}\rangle_{AB}=\frac{1}{2}\left(|00\rangle-|11\rangle+|22\rangle-|33\rangle\right)_{AB},\tag{45}$$

$$|\psi_{2,1}\rangle_{AB}=\frac{1}{2}\left(|01\rangle-|12\rangle+|23\rangle-|30\rangle\right)_{AB},\tag{46}$$

$$|\psi_{2,2}\rangle_{AB}=\frac{1}{2}\left(|02\rangle-|13\rangle+|20\rangle-|31\rangle\right)_{AB},\tag{47}$$

$$|\psi_{2,3}\rangle_{AB}=\frac{1}{2}\left(|03\rangle-|10\rangle+|21\rangle-|32\rangle\right)_{AB},\tag{48}$$

$$|\psi_{3,0}\rangle_{AB}=\frac{1}{2}\left(|00\rangle-\mathrm{i}|11\rangle-|22\rangle+\mathrm{i}|33\rangle\right)_{AB},\tag{49}$$

$$|\psi_{3,1}\rangle_{AB}=\frac{1}{2}\left(|01\rangle-\mathrm{i}|12\rangle-|23\rangle+\mathrm{i}|30\rangle\right)_{AB},\tag{50}$$

$$|\psi_{3,2}\rangle_{AB}=\frac{1}{2}\left(|02\rangle-\mathrm{i}|13\rangle-|20\rangle+\mathrm{i}|31\rangle\right)_{AB},\tag{51}$$

$$|\psi_{3,3}\rangle_{AB}=\frac{1}{2}\left(|03\rangle-\mathrm{i}|10\rangle-|21\rangle+\mathrm{i}|32\rangle\right)_{AB}.\tag{52}$$

Then, $\mathcal{S}^4$ transforms the generalized Bell states $\{|\psi_{i,j}\rangle_{AB}\}$ into

$$\mathcal{S}^4|\mathcal{H}_0\rangle^c|\psi_{0,0}\rangle_{AB}=|\mathcal{H}_0\rangle^c\otimes|\psi_{0,1}\rangle_{AB},\tag{53}$$

$$\mathcal{S}^4|\mathcal{H}_0\rangle^c|\psi_{0,1}\rangle_{AB}=|\mathcal{H}_0\rangle^c\otimes|\psi_{0,2}\rangle_{AB},\tag{54}$$

$$\mathcal{S}^4|\mathcal{H}_0\rangle^c|\psi_{0,2}\rangle_{AB}=|\mathcal{H}_0\rangle^c\otimes|\psi_{0,3}\rangle_{AB},\tag{55}$$

$$\mathcal{S}^4|\mathcal{H}_0\rangle^c|\psi_{0,3}\rangle_{AB}=|\mathcal{H}_0\rangle^c\otimes|\psi_{0,0}\rangle_{AB},\tag{56}$$

$$\mathcal{S}^4|\mathcal{H}_0\rangle^c|\psi_{1,0}\rangle_{AB}=|\mathcal{H}_3\rangle^c\otimes|\psi_{1,1}\rangle_{AB},\tag{57}$$

$$\mathcal{S}^4|\mathcal{H}_0\rangle^c|\psi_{1,1}\rangle_{AB}=|\mathcal{H}_3\rangle^c\otimes|\psi_{1,2}\rangle_{AB},\tag{58}$$

$$\mathcal{S}^4|\mathcal{H}_0\rangle^c|\psi_{1,2}\rangle_{AB}=|\mathcal{H}_3\rangle^c\otimes|\psi_{1,3}\rangle_{AB},\tag{59}$$

$$\mathcal{S}^4|\mathcal{H}_0\rangle^c|\psi_{1,3}\rangle_{AB}=|\mathcal{H}_3\rangle^c\otimes|\psi_{1,0}\rangle_{AB},\tag{60}$$

$$\mathcal{S}^4|\mathcal{H}_0\rangle^c|\psi_{2,0}\rangle_{AB}=|\mathcal{H}_2\rangle^c\otimes|\psi_{2,1}\rangle_{AB},\tag{61}$$

$$\mathcal{S}^4|\mathcal{H}_0\rangle^c|\psi_{2,1}\rangle_{AB}=|\mathcal{H}_2\rangle^c\otimes|\psi_{2,2}\rangle_{AB},\tag{62}$$

$$\mathcal{S}^4|\mathcal{H}_0\rangle^c|\psi_{2,2}\rangle_{AB}=|\mathcal{H}_2\rangle^c\otimes|\psi_{2,3}\rangle_{AB},\tag{63}$$

Table 2. The correspondences between the outcome of the quantum 4-switch $\mathcal{S}^4$, ququart information, and the state transition for discriminating sixteen Bell states.

Outcome of 4-switch $\mathcal{S}^4$	Ququart information of (j_A, j_B)	Output Bell state	Input Bell state
$\|\mathcal{H}_0\rangle^c$	$j_B = (j_A+1) \bmod 4$	$\|\psi_{0,1}\rangle_{AB}$	$\|\psi_{0,0}\rangle_{AB}$
	$j_B = (j_A+2) \bmod 4$	$\|\psi_{0,2}\rangle_{AB}$	$\|\psi_{0,1}\rangle_{AB}$
	$j_B = (j_A+3) \bmod 4$	$\|\psi_{0,3}\rangle_{AB}$	$\|\psi_{0,2}\rangle_{AB}$
	$j_A = j_B$	$\|\psi_{0,0}\rangle_{AB}$	$\|\psi_{0,3}\rangle_{AB}$
$\|\mathcal{H}_3\rangle^c$	$j_B = (j_A+1) \bmod 4$	$\|\psi_{1,1}\rangle_{AB}$	$\|\psi_{1,0}\rangle_{AB}$
	$j_B = (j_A+2) \bmod 4$	$\|\psi_{1,2}\rangle_{AB}$	$\|\psi_{1,1}\rangle_{AB}$
	$j_B = (j_A+3) \bmod 4$	$\|\psi_{1,3}\rangle_{AB}$	$\|\psi_{1,2}\rangle_{AB}$
	$j_A = j_B$	$\|\psi_{1,0}\rangle_{AB}$	$\|\psi_{1,3}\rangle_{AB}$
$\|\mathcal{H}_2\rangle^c$	$j_B = (j_A+1) \bmod 4$	$\|\psi_{2,1}\rangle_{AB}$	$\|\psi_{2,0}\rangle_{AB}$
	$j_B = (j_A+2) \bmod 4$	$\|\psi_{2,2}\rangle_{AB}$	$\|\psi_{2,1}\rangle_{AB}$
	$j_B = (j_A+3) \bmod 4$	$\|\psi_{2,3}\rangle_{AB}$	$\|\psi_{2,2}\rangle_{AB}$
	$j_A = j_B$	$\|\psi_{2,0}\rangle_{AB}$	$\|\psi_{2,3}\rangle_{AB}$
$\|\mathcal{H}_1\rangle^c$	$j_B = (j_A+1) \bmod 4$	$\|\psi_{3,1}\rangle_{AB}$	$\|\psi_{3,0}\rangle_{AB}$
	$j_B = (j_A+2) \bmod 4$	$\|\psi_{3,2}\rangle_{AB}$	$\|\psi_{3,1}\rangle_{AB}$
	$j_B = (j_A+3) \bmod 4$	$\|\psi_{3,3}\rangle_{AB}$	$\|\psi_{3,2}\rangle_{AB}$
	$j_A = j_B$	$\|\psi_{3,0}\rangle_{AB}$	$\|\psi_{3,3}\rangle_{AB}$

$$\mathcal{S}^4|\mathcal{H}_0\rangle^c|\psi_{2,3}\rangle_{AB} = |\mathcal{H}_2\rangle^c \otimes |\psi_{2,0}\rangle_{AB}, \tag{64}$$

$$\mathcal{S}^4|\mathcal{H}_0\rangle^c|\psi_{3,0}\rangle_{AB} = |\mathcal{H}_1\rangle^c \otimes |\psi_{3,1}\rangle_{AB}, \tag{65}$$

$$\mathcal{S}^4|\mathcal{H}_0\rangle^c|\psi_{3,1}\rangle_{AB} = |\mathcal{H}_1\rangle^c \otimes |\psi_{3,2}\rangle_{AB}, \tag{66}$$

$$\mathcal{S}^4|\mathcal{H}_0\rangle^c|\psi_{3,2}\rangle_{AB} = |\mathcal{H}_1\rangle^c \otimes |\psi_{3,3}\rangle_{AB}, \tag{67}$$

$$\mathcal{S}^4|\mathcal{H}_0\rangle^c|\psi_{3,3}\rangle_{AB} = |\mathcal{H}_1\rangle^c \otimes |\psi_{3,0}\rangle_{AB}. \tag{68}$$

Based on equations (37)–(68), one can see that the sixteen generalized Bell states can be completely heralded by the outcomes of the quantum 4-switch $\mathcal{S}^4$, Alice, and Bob, see table 2.

2.4. Deterministic BSA in d-dimensional system via ICO d-switch

Our approach can also be extended to arbitrary d-dimensional (qudit, i.e. $d>4$ system) scenario. The ICO d-switch $\mathcal{S}^d$ operation can be written as

$$\begin{aligned}\mathcal{S}^d|\mathcal{D}_0\rangle^c|\varphi_1\rangle_A^t|\varphi_2\rangle_B = \frac{1}{\sqrt{d}}\big(&|0\rangle^c \otimes U_1^d|\varphi_1\rangle_A^t \otimes V_1^d|\varphi_2\rangle_B^t + |1\rangle^c \otimes U_2^d|\varphi_1\rangle_A^t \otimes V_2^d|\varphi_2\rangle_B^t \\ &+ \cdots + |d-1\rangle^c \otimes U_d^d|\varphi_1\rangle_A^t \otimes V_d^d|\varphi_2\rangle_B^t\big).\end{aligned} \tag{69}$$

Here and henceforth,

$$|\mathcal{D}_i\rangle^c = \frac{1}{\sqrt{d}}\left(\omega^{0\cdot i}|0\rangle^c + \omega^{1\cdot i}|1\rangle^c + \cdots + \omega^{(d-1)\cdot i}|d-1\rangle^c\right), \quad i = 0,1,\cdots,(d-1). \tag{70}$$

If the embedded local qudit operations U_k^d and V_k^d with $k = 1,2,\cdots,d$ within $\mathcal{S}^d$ are adjusted as

$$U_k^d = \left(U_{\text{shift}}^d\right)^{k-1}, \quad V_k^d = \left(U_{\text{shift}}^d\right)^k, \tag{71}$$

where

$$U_{\text{shift}}^d = \begin{pmatrix} 0 & 0 & \dots & 0 & 1 \\ 1 & 0 & \dots & 0 & 0 \\ 0 & 1 & \ddots & \vdots & \vdots \\ \vdots & \ddots & \ddots & 0 & 0 \\ 0 & \dots & 0 & 1 & 0 \end{pmatrix}_{d\times d}. \tag{72}$$

Then, the evolutions of a set of generalized Bell states $\{|\varphi_{i,j}\rangle\}$ in d-dimensional system induced by $\mathcal{S}^d$ can be written as

$$\mathcal{S}^d|\mathcal{D}_0\rangle^c|\varphi_{i,j}\rangle_{AB} = |\mathcal{D}_{(d-i) \bmod d}\rangle^c \otimes |\varphi_{i,(j+1) \bmod d}\rangle_{AB}, \tag{73}$$

where

$$|\varphi_{i,j}\rangle_{AB} = \frac{1}{\sqrt{d}}\sum_{k=0}^{d-1}\omega^{ik}|k\rangle_A|(k+j) \bmod d\rangle_B, \;\; i,j \in \{0,1,\ldots,(d-1)\} \text{ and } \omega = \mathrm{e}^{\frac{2\pi \mathrm{i}}{d}}. \tag{74}$$

Based on equation (73), one can see that regardless of the system dimension d, the d^2 generalized Bell states can be divided into d distinguishable groups, $\{|\varphi_{i,0}\rangle_{AB}, |\varphi_{i,1}\rangle_{AB}, \cdots, |\varphi_{i,(d-1)}\rangle_{AB}\}$ corresponding to $|\mathcal{D}_{(d-i) \bmod d}\rangle^c$, $i = 0,1,\cdots,(d-1)$. Subsequently, the particles held by Alice and Bob are measured in the basis $\{|0\rangle,|1\rangle,\cdots,|d-1\rangle\}$, respectively. Based on the measured results, the states in each group can be distinguished from each other perfectly.

We further find that, after the d-switch process, the indefinite causal structure of the quantum switch does not get consumed. Hence the nondestructive BSA can be achieved by iterating the d-switch process for two rounds.

3. Physical implementation of BSA in d-dimensional system via gravitational ICO switch

The ICO switch $\mathcal{S}^d$ is the key element of our high-dimensional BSA protocols. It is known that space-time physics [50], causal modeling [35], time-delocalization [51], and time-direction [32] are the viable candidates for quantum switch. Inspired by the gravitational ICO quantum 2-switch proposed in [24], we will introduce the working principle of gravitational (space-time) ICO quantum d-switch $\mathcal{S}^d$ for implementing our high-dimensional BSA protocols.

3.1. The gravitational ICO 3-switch $\mathcal{S}^3$ for BSA in 3-dimensional system

We now detail how the ICO 3-switch $\mathcal{S}^3$ mechanism (shown in section 2.2) can be implemented utilizing the gravitational effects induced by the matter-energy distribution.

Consider two initially synchronized clocks (agents), Alice and Bob, placed in the gravitational field of a massive object M. r_A (r_B) is the spatial distance between the mass and Alice (Bob). Consider three events: Event A, defined by Alice's clock at her local time τ. Events B_1 and B_2, defined by Bob's clock at his local times τ and τ_1, respectively. Here $\tau_1 > \tau$, that is, B_1 and B_2 are always in the fixed order, i.e. B_1 is always in the causal past of B_2 ($B_1 \to B_2$).

In general relativity, time passes more slowly closer to the massive object due to gravitational time dilation. Note that a physical system can only be transferred from the past to the future, but not the other way around.

As shown in table 3, depending on the geometry of the mass object, there are three types of causal orders (after local operation is completed, the agent will send the light signals to each other):

(1) Configuration $M_{B_1\to B_2\to A}$. As shown in figure 1(a), Alice's clock is located near the mass object ($r_A = R_1$, $r_B = R_1 + h$). The gravitational time dilation results in the causal order $B_1 \to B_2 \to A$. Consequently, event A lies in the future light cone of event B_2. The corresponding unitary operations performed at the space-time events B_1, B_2, and A are $U^3_{B_1}$, $U^3_{B_2}$, and $U^3_{A|B_2}$, respectively.
(2) Configuration $M_{B_1\to A\to B_2}$. For this configuration, shown in figure 1(b), the clocks are positioned such that $r_A = R_2 > R_1$ and $r_B = R_2 + h$. This arrangement leads to the causal order $B_1 \to A \to B_2$. Therefore, event A lies in the future light cone of event B_1, and event B_2 lies in the future light cone of event A. The unitary operations performed at the spacetime events B_1, A, and B_2 are $U^3_{B_1}$, $U^3_{A|B_1}$, and $U^3_{B_2|A}$, respectively.
(3) Configuration $M_{A\to B_1\to B_2}$. In the third configuration, shown in figure 1(c), Bob's clock is closer to the mass object ($r_B = R_1$, $r_A = R_1 + h$), resulting in the causal order $A \to B_1 \to B_2$. This means both events B_1 and B_2 lie in the future light cone of event A. The corresponding unitary operations performed at the spacetime events A, B_1, and B_2 are U^3_A, $U^3_{B_1|A}$, and $U^3_{B_2|A}$, respectively.

Note that the causal structure of the space-time, as shown in figure 1, is definite. Fortunately, the quantum superposition of three distinct locations

$$|\mathcal{F}_0\rangle^c = \frac{1}{\sqrt{3}}\left(|M_{B_1\to B_2\to A}\rangle + |M_{B_1\to A\to B_2}\rangle + |M_{A\to B_1\to B_2}\rangle\right) \tag{75}$$

Table 3. The correspondence between the signal and operation in each configuration in 3-dimensional quantum system.

Agent	Configuration	Scenario	Operation
Alice	$\|M_{B_1\to B_2\to A}\rangle$	Alice receives Bob's signals b_1 and b_2 before $t_A=\tau$	$U^3_{A\|B_2}$
	$\|M_{B_1\to A\to B_2}\rangle$	Alice receives Bob's signal b_1 only before $t_A=\tau$	$U^3_{A\|B_1}$
	$\|M_{A\to B_1\to B_2}\rangle$	No signal received before $t_A=\tau$	U^3_A
Bob	$\|M_{B_1\to B_2\to A}\rangle$	No signal received before $t_B=\tau_1$	$U^3_{B_2}U^3_{B_1}$
	$\|M_{B_1\to A\to B_2}\rangle$	Bob only receives Alice's signal a received before $t_B=\tau_1$	$U^3_{B_2\|A}U^3_{B_1}$
	$\|M_{A\to B_1\to B_2}\rangle$	Bob receives Alice's signals a before $t_B=\tau$	$U^3_{B_2\|A}U^3_{B_1\|A}$

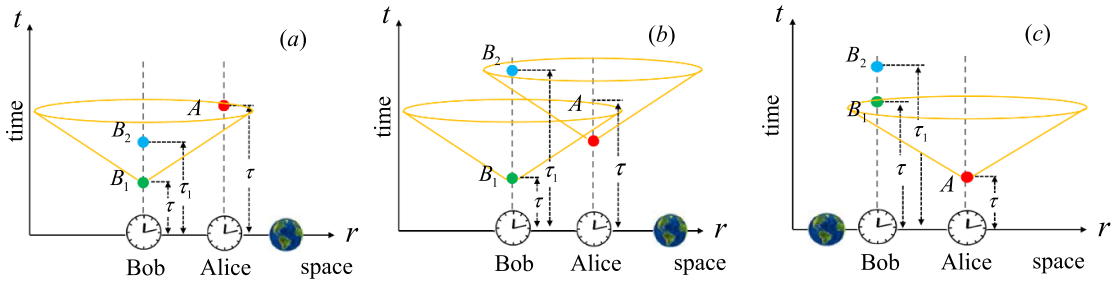

Figure 1. Quantum control of temporal order for constructing gravitational ICO 3-switch $\mathcal{S}^3$. (a) Alice's clock is located near the mass object with $r_A=R_1$ and $r_B=R_1+h$. Events B_1, B_2, and A will occur in succession, i.e. $M_{B_1\to B_2\to A}$. (b) Alice's clock is located near the mass object with $r_A=R_2>R_1$ and $r_B=R_2+h$. Events B_1, A, and B_2 will occur in succession, i.e. $M_{B_1\to A\to B_2}$. (c) Bob's clock is located near the mass object with $r_B=R_1$ and $r_A=R_1+h$. Events A, B_1, and B_2 will occur in succession, i.e. $M_{A\to B_1\to B_2}$. r_A (r_B) is the spatial distance between the mass and Alice (Bob).

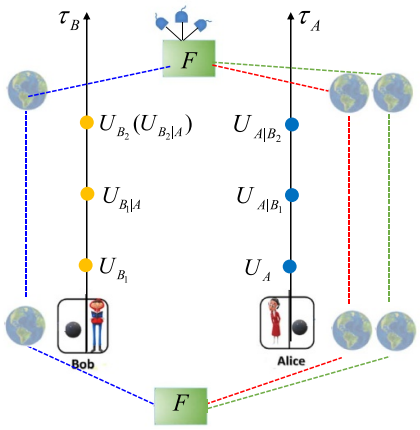

Figure 2. The gravitational ICO 3-switch $\mathcal{S}^3$. U^3_A, $U^3_{B_1}$, $U^3_{B_2}$, $U^3_{B_1|A}$, $U^3_{B_2|A}$, $U^3_{A|B_1}$, $U^3_{B_1|A}$, and $U^3_{B_2|A}$ are the local single-qutrit unitary operations.

is the result of a process wherein the order of operation performed on the target system is determined by the position of the mass object. The operation of this gravitational ICO 3-switch $\mathcal{S}^3$ depicted in figure 2 can be written as

$$\begin{aligned}\mathcal{S}^3|\Psi\rangle^t_A|\Psi\rangle^t_B|\mathcal{F}_0\rangle^c=\frac{1}{\sqrt{3}}\Big(&|M_{B_1\to B_2\to A}\rangle\left(U^3_{A|B_2}\right)|\Psi\rangle^t_A\otimes\left(U^3_{B_2}U^3_{B_1}\right)|\Psi\rangle^t_B\\&+|M_{B_1\to A\to B_2}\rangle\left(U^3_{A|B_1}\right)|\Psi\rangle^t_A\otimes\left(U^3_{B_2|A}U^3_{B_1}\right)|\Psi\rangle^t_B\\&+|M_{A\to B_1\to B_2}\rangle\left(U^3_A\right)|\Psi\rangle^t_A\otimes\left(U^3_{B_2|A}U^3_{B_1|A}\right)|\Psi\rangle^t_B\Big).\end{aligned}\tag{76}$$

The state $|\mathcal{F}_0\rangle^c$, given in equations (5)–(7), can be identified as the control qutrit of the gravitational ICO 3-switch as it coherently governs the order of operations acting on the target system.

Table 4. The correspondence between the signal and operation in each configuration in 4-dimensional quantum system.

Agent	Configuration	Scenario	Operation
Alice	$\|M_{B_1\to B_2\to B_3\to A}\rangle$	Received Bob's b_1, b_2 and b_3 signals before $t_A=\tau^*$	$U^4_{A\|B_3}$
	$\|M_{B_1\to B_2\to A\to B_3}\rangle$	Received Bob's b_1, b_2 signals before $t_A=\tau^*$	$U^4_{A\|B_2}$
	$\|M_{B_1\to A\to B_2\to B_3}\rangle$	Received Bob's b_1 signal before $t_A=\tau^*$	$U^4_{A\|B_1}$
	$\|M_{A\to B_1\to B_2\to B_3}\rangle$	No signal received before $t_A=\tau^*$	U^4_A
Bob	$\|M_{B_1\to B_2\to B_3\to A}\rangle$	No signal received before $t_B=\tau_2^*$	$U^4_{B_3}U^4_{B_2}U^4_{B_1}$
	$\|M_{B_1\to B_2\to A\to B_3}\rangle$	No signal received before $t_B=\tau_1^*$, but Alice's signals received before $t_B=\tau_2^*$	$U^4_{B_3\|A}U^4_{B_2}U^4_{B_1}$
	$\|M_{B_1\to A\to B_2\to B_3}\rangle$	No signal received before $t_B=\tau^*$, but Alice's signals received before $t_B=\tau_1^*$	$U^4_{B_3\|A}U^4_{B_2\|A}U^4_{B_1}$
	$\|M_{A\to B_1\to B_2\to B_3}\rangle$	Alice's signals received before $t_B=\tau^*$	$U^4_{B_3\|A}U^4_{B_2\|A}U^4_{B_1\|A}$

The correspondences between equations (4) and (76) are

$$|M_{B_1\to B_2\to A}\rangle\equiv|0\rangle^c,\ \ |M_{B_1\to A\to B_2}\rangle\equiv|1\rangle^c,\ \ |M_{A\to B_1\to B_2}\rangle\equiv|2\rangle^c, \tag{77}$$

$$U^3_{A|B_2}\equiv U^3_1,\ \ U^3_{A|B_1}\equiv U^3_2,\ \ U^3_A\equiv U^3_3, \tag{78}$$

$$U^3_{B_2}U^3_{B_1}\equiv V^3_1,\ \ U^3_{B_2|A}U^3_{B_1}\equiv V^3_2,\ \ U^3_{B_2|A}U^3_{B_1|A}\equiv V^3_3, \tag{79}$$

where

$$U^3_{A|B_1}=U^3_{\rm shift},\quad U^3_A=U^3_{B_1}=U^3_{B_2}=\left(U^3_{\rm shift}\right)^2,\quad U^3_{B_1|A}=U^3_{B_2|A}=U^3_{A|B_2}=I_3. \tag{80}$$

3.2. The gravitational ICO 4-switch $\mathcal{S}^4$ for BSA in 4-dimensional system

As shown in figure 3, we consider four events: Event A, defined by Alice's clock at time τ^*. Events B_1, B_2, and B_3, defined by Bob's clock at times τ^*, τ_1^*, and τ_2^*, respectively. Here $\tau_2^*>\tau_1^*>\tau^*$. As shown in table 4, the four types of causal orders are:

(1) Configuration $M_{B_1\to B_2\to B_3\to A}$. As shown in figure 3(a), the corresponding order of unitary operations performed by two agents is $U^4_{B_1}$, $U^4_{B_2}$, $U^4_{B_3}$, and $U^4_{A|B_3}$.
(2) Configuration $M_{B_1\to B_2\to A\to B_3}$. As shown in figure 3(b), the corresponding order of unitary operations performed by two agents is $U^4_{B_1}$, $U^4_{B_2}$, $U^4_{A|B_1}$, and $U^4_{B_3|A}$.
(3) Configuration $M_{B_1\to A\to B_2\to B_3}$. As shown in figure 3(c), the corresponding order of unitary operations performed by two agents is $U^4_{B_1}$, $U^4_{A|B_1}$, $U^4_{B_2|A}$, and $U^4_{B_3|A}$.
(4) Configuration $M_{A\to B_1\to B_2\to B_3}$. As shown in figure 3(d), the corresponding order of unitary operations performed by two agents is U^4_A, $U^4_{B_1|A}$, $U^4_{B_2|A}$, and $U^4_{B_3|A}$.

Therefore, the operation of the gravitational ICO 4-switch $\mathcal{S}^4$, depicted in figure 4, can be expressed as

$$\begin{aligned}\mathcal{S}^4|\psi\rangle^t_A|\psi\rangle^t_B|\mathcal{H}_0\rangle^c=\frac{1}{2}\Big(&|M_{B_1\to B_2\to B_3\to A}\rangle\left(U^4_{A|B_3}\right)|\psi\rangle^t_A\otimes\left(U^4_{B_3}U^4_{B_2}U^4_{B_1}\right)|\psi\rangle^t_B\\&+|M_{B_1\to B_2\to A\to B_3}\rangle\left(U^4_{A|B_2}\right)|\psi\rangle^t_A\otimes\left(U^4_{B_3|A}U^4_{B_2}U^4_{B_1}\right)|\psi\rangle^t_B\\&+|M_{B_1\to A\to B_2\to B_3}\rangle\left(U^4_{A|B_1}\right)|\psi\rangle^t_A\otimes\left(U^4_{B_3|A}U^4_{B_2|A}U^4_{B_1}\right)|\psi\rangle^t_B\\&+|M_{A\to B_1\to B_2\to B_3}\rangle\left(U^4_A\right)|\psi\rangle^t_A\otimes\left(U^4_{B_3|A}U^4_{B_2|A}U^4_{B_1|A}\right)|\psi\rangle^t_B\Big).\end{aligned} \tag{81}$$

The correspondences between equations (29) and (81) are

$$\begin{aligned}&|M_{B_1\to B_2\to B_3\to A}\rangle\equiv|0\rangle^c,\ \ |M_{B_1\to B_2\to A\to B_3}\rangle\equiv|1\rangle^c,\\&|M_{B_1\to A\to B_2\to B_3}\rangle\equiv|2\rangle^c,\ \ |M_{A\to B_1\to B_2\to B_3}\rangle\equiv|3\rangle^c,\end{aligned} \tag{82}$$

$$U^4_{A|B_3}\equiv U^4_1,\ \ U^4_{A|B_2}\equiv U^4_2,\ \ U^4_{A|B_1}\equiv U^4_3,\ \ U^4_A\equiv U^4_4, \tag{83}$$

$$U^4_{B_3}U^4_{B_2}U^4_{B_1}\equiv V^4_1,\ U^4_{B_3|A}U^4_{B_2}U^4_{B_1}\equiv V^4_2,\ U^4_{B_3|A}U^4_{B_2|A}U^4_{B_1}\equiv V^4_3,\ U^4_{B_3|A}U^4_{B_2|A}U^4_{B_1|A}\equiv V^4_4, \tag{84}$$

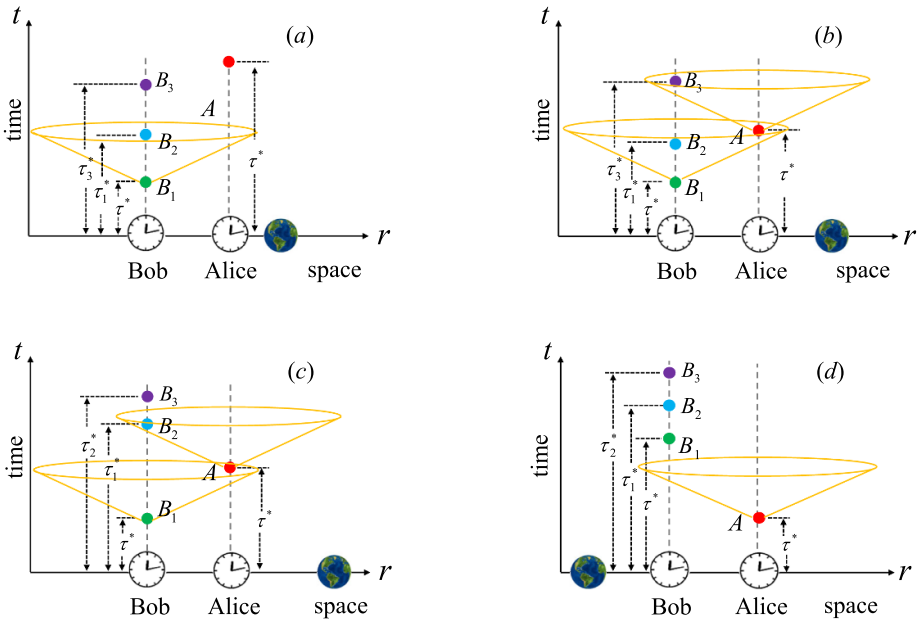

Figure 3. Quantum control of temporal order for gravitational ICO 4-switch $\mathcal{S}^4$. (a) The space-time geometry is $M_{B_1\to B_2\to B_3\to A}$. (b) The space-time geometry is $M_{B_1\to B_2\to A\to B_3}$. (c) The space-time geometry is $M_{B_1\to A\to B_2\to B_3}$. (d) The space-time geometry is $M_{A\to B_1\to B_2\to B_3}$,

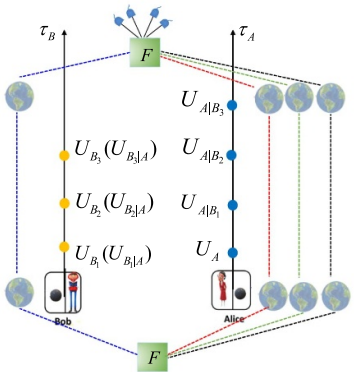

Figure 4. The gravitational ICO 4-switch $\mathcal{S}^4$. U_A^4, $U_{B_1}^4$, $U_{B_2}^4$, $U_{B_3}^4$, $U_{B_1|A}^4$, $U_{B_2|A}^4$, $U_{B_3|A}^4$, $U_{A|B_1}^4$, $U_{A|B_2}^4$, and $U_{A|B_3}^4$ are the embedded local single-ququart unitary operations.

where

$$U_{A|B_2}^4 = U_{\text{shift}}^4, \quad U_{A|B_1}^4 = \left(U_{\text{shift}}^4\right)^2, \tag{85}$$

$$U_{B_1}^4 = U_{B_2}^4 = U_{B_2}^4 = U_A^4 = \left(U_{\text{shift}}^4\right)^3, \tag{86}$$

$$U_{B_1|A}^4 = U_{B_2|A}^4 = U_{B_3|A}^4 = U_{A|B_3}^4 = I_4. \tag{87}$$

3.3. The gravitational ICO d-switch $\mathcal{S}^d$ for BSA in d-dimensional system

As shown in figure 5, consider there are d ($d>4$) events A, B_1, B_2, $\cdots$, B_{d-1}. There are d types of causal orders:

(1) Configuration $M_{B_1\to B_2\to\cdots\to B_{d-1}\to A}$. The order of unitary operations performed by the two agents is $U_{B_1}^d$, $U_{B_2}^d$, $\cdots$, $U_{B_{d-1}}^d$, and $U_{A|B_{d-1}}^d$.
(2) Configuration $M_{B_1\to B_2\to\cdots\to A\to B_{d-1}}$. The order of unitary operations performed by the two agents is $U_{B_1}^d$, $\cdots$, $U_{B_{d-2}}^d$, $U_{A|B_{d-2}}^d$, and $U_{B_{d-1}|A}^d$.
...

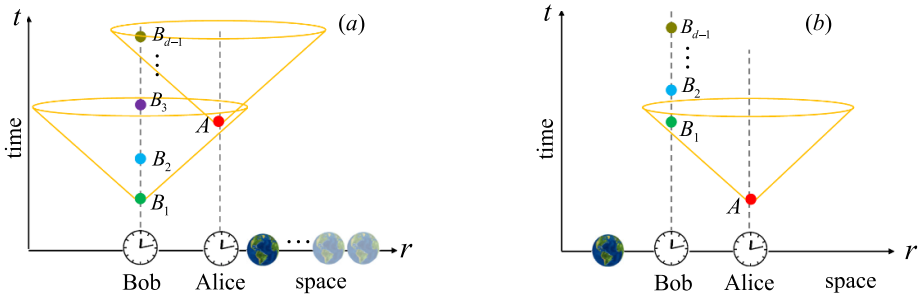

Figure 5. Quantum control of temporal order for gravitational ICO d-switch $\mathcal{S}^d$. (a) Alice's clock is located near the mass object. (b) Bob's clock is located near the mass object.

(d) Configuration $M_{A\to B_1\to B_2\to\cdots\to B_{d-1}}$. The order of unitary operations performed by the two agents is U^d_A, $U^d_{B_1|A}$, $U^d_{B_2|A}$, $\cdots$, $U^d_{B_{d-1}|A}$.

The physically allowed mass configuration of gravitational ICO d-switch $\mathcal{S}^d$ can be given by

$$\begin{aligned}|\mathcal{D}_0\rangle^c = \frac{1}{\sqrt{d}}\big(&|M_{B_1\to B_2\to\cdots\to B_{d-1}\to A}\rangle + |M_{B_1\to B_2\to\cdots\to A\to B_{d-1}}\rangle \\ &+\cdots+|M_{A\to B_1\to B_2\to\cdots\to B_{d-1}}\rangle\big).\end{aligned} \tag{88}$$

Hence the transformation of the d-switch $\mathcal{S}^d$ depicted in figure 6 can be written as

$$\begin{aligned}\mathcal{S}^d|\varphi\rangle^t_A|\varphi\rangle^t_B|\mathcal{D}_0\rangle^c = \frac{1}{\sqrt{d}}\Big(&|M_{B_1\to B_2\to\cdots\to B_{d-1}\to A}\rangle\left(U^d_{A|B_{d-1}}\right)|\varphi\rangle^t_A\otimes\left(U^d_{B_{d-1}}U^d_{B_{d-2}}\cdots U^d_{B_1}\right)|\varphi\rangle^t_B \\ &+|M_{B_1\to B_2\to\cdots\to A\to B_{d-1}}\rangle\left(U^d_{A|B_{d-2}}\right)|\varphi\rangle^t_A\otimes\left(U^d_{B_{d-1}|A}U^d{}_{B_{d-2}}\cdots U^d_{B_1}\right)|\varphi\rangle^t_B \\ &+\cdots \\ &+|M_{A\to B_1\to B_2\to\cdots\to B_{d-1}}\rangle\left(U^d_A\right)|\varphi\rangle^t_A\otimes\left(U^d_{B_{d-1}|A}U^d_{B_{d-2}|A}\cdots U^d_{B_1|A}\right)|\varphi\rangle^t_B\Big).\end{aligned} \tag{89}$$

The correspondences between equations (69) and (89) are

$$\begin{aligned}&|M_{B_1\to B_2\to\cdots\to B_{d-1}\to A}\rangle \equiv |0\rangle^c,\\ &|M_{B_1\to B_2\to\cdots\to A\to B_{d-1}}\rangle \equiv |1\rangle^c,\\ &\cdots\\ &|M_{A\to B_1\to B_2\to\cdots\to B_{d-1}}\rangle \equiv |d-1\rangle^c,\end{aligned} \tag{90}$$

$$U^d_{A|B_{d-1}} \equiv U^d_1,\ \ U^d_{A|B_{d-2}} \equiv U^d_2,\ \ \ldots,\ \ U^d_A \equiv U^d_d, \tag{91}$$

$$U^d_{B_{d-1}}U^d_{B_{d-2}}\cdots U^d_{B_1} \equiv V^d_1,\ \ U^d_{B_{d-1}|A}U^d_{B_{d-2}}\cdots U^d_{B_1} \equiv V^d_2,\ \ U^d_{B_{d-1}|A}U^d_{B_{d-2}|A}\cdots U^d_{B_1|A} \equiv V^d_d, \tag{92}$$

where

$$U^d_A = \left(U^d_{\text{shift}}\right)^{d-1},\ \ U^d_{A|B_1} = \left(U^d_{\text{shift}}\right)^{d-2},\ \ \cdots,\ \ U^d_{A|B_k} = \left(U^d_{\text{shift}}\right)^{d-1-k},\ \ \cdots,\ \ U^d_{A|B_{d-1}} = I_d, \tag{93}$$

$$U^d_{B_1|A} = U^d_{B_2|A} = \cdots = U^d_{B_{d-1}|A} = I_d, \tag{94}$$

$$U^d_{B_1} = \left(U^d_{\text{shift}}\right)^{d-1}, \tag{95}$$

$$U^d_{B_2} = U^d_{B_3} = \cdots = U^d_{B_{d-1}} = \left(U^d_{\text{shift}}\right)^{d-1}. \tag{96}$$

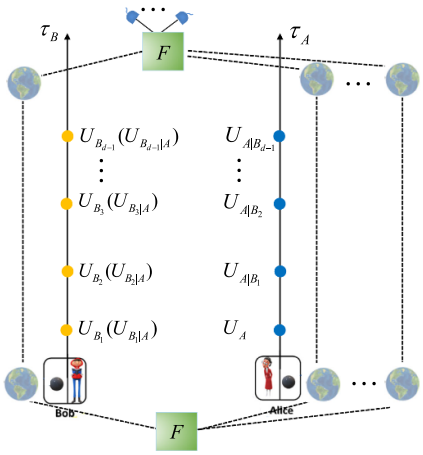

Figure 6. The gravitational ICO d-switch $\mathcal{S}^d$. U_A^d, $U_{B_1}^d$, $U_{B_2}^d$, $\cdots$, $U_{B_{d-1}}^d$, $U_{B_1|A}^d$, $U_{B_2|A}^d$, $\cdots$, $U_{B_{d-1}|A}^d$, $U_{A|B_1}^d$, $U_{A|B_2}$, $\cdots$, $U_{A|B_{d-1}}^d$ are the inherent local single-qudit unitary operations.

4. Discussion and conclusion

ICO serves as a universal resource for locally implementing various QIP tasks on spatially distributed quantum systems, and ICO has mainly focused on 2-dimensional quantum systems. By exploiting solely single-qubit operations in superposition of causal orders, the task can be completed without entangled gates or direct interaction between qubits. While this resource has been applied to high-dimensional tasks such as quantum teleportation [24], a complete and deterministic high-dimensional Bell-state analysis (BSA) has remained a largely open problem.

In this paper, we proposed complete and deterministic BSA protocols beyond qubit systems via ICO. We first proposed a ICO quantum 3-switch $\mathcal{S}^3$, and a perfect $\mathcal{S}^3$-based BSA protocol in 3-dimensional quantum system is proposed. Subsequently, our approach is extended to 4-dimensional and arbitrary d-dimensional scenarios. Furthermore, the gravitational ICO 3-switch, ICO 4-switch, and even ICO d-switch are designed to complete our BSA schemes. The results indicate that, independent of the dimension, perfect one-shot qudit BSA can be achieved via ICO quantum d-switch $\mathcal{S}^d$ with $d \geqslant 3$). Maximally entangled states or controlled-unitary gates, which are necessary for previous BSA protocols, are not required in our scheme. In standard two-step BSA protocols, the bit and phase information of the Bell states are distinguished sequentially. Importantly, in our schemes, the nondestructive BSAs can also be achieved by iterating the d-switch process for two rounds. Additionally, the intrinsic local unitary operations involved in the gravitational ICO switch are remarkably simple, consisting solely of shift gates.

Data availability statement

No new data were created or analysed in this study.

Acknowledgments

This work is supported by the National Natural Science Foundation of China under Grant Nos. 62371038 and 12505028, the Science Research Project of Hebei Education Department under Grant No. QN2025054, the Beijing Natural Science Foundation under Grant No. 4252006, and the Fundamental Research Funds for the Central Universities under Grant No. FRF-TP-19-011A3.

ORCID iDs

Jun-Hai Zhao 0009-0008-2193-8299
Wen-Qiang Liu 0000-0001-9804-2716
Hai-Rui Wei 0000-0001-7459-4161

References

[1] Ekert A K 1991 Quantum cryptography based on Bell's theorem *Phys. Rev. Lett.* **67** 661
[2] Liu J, Lin Z, Liu D, Feng X, Liu F, Cui K, Huang Y and Zhang W 2023 High-dimensional quantum key distribution using energy-time entanglement over 242 km partially deployed fiber *Quantum Sci. Technol.* **9** 015003
[3] Bennett C H and Wiesner S J 1992 Communication via one-and two-particle operators on Einstein-Podolsky-Rosen states *Phys. Rev. Lett.* **69** 2881
[4] Guo H, Liu N, Li Z, Yang R, Sun H, Liu K and Gao J 2022 Generation of continuous-variable high-dimensional entanglement with three degrees of freedom and multiplexing quantum dense coding *Photon. Res.* **10** 2828
[5] Bennett C H, Brassard G, Crépeau C, Jozsa R, Peres A and Wootters W K 1993 Teleporting an unknown quantum state via dual classical and Einstein-Podolsky-Rosen channels *Phys. Rev. Lett.* **70** 1895
[6] Hu X-M, Guo Y, Liu B-H, Li C-F and Guo G-C 2023 Progress in quantum teleportation *Nat. Rev. Phys.* **5** 339
[7] Hillery M, Bužek V and Berthiaume A 1999 Quantum secret sharing *Phys. Rev. A* **59** 1829
[8] Karlsson A, Koashi M and Imoto N 1999 Quantum entanglement for secret sharing and secret splitting *Phys. Rev. A* **59** 162
[9] Zukowski M, Zeilinger A, Horne M and Ekert A K 1993 Event-ready-detectors Bell experiment via entanglement swapping *Phys. Rev. Lett.* **71** 4287
[10] Zhao H and Shan C 2024 Robustness and symmetry of deterministic quantum entanglement swapping *Phys. Rev. A* **110** 032618
[11] Kwiat P G and Weinfurter H 1998 Embedded Bell state analysis *Phys. Rev. A* **58** R2623
[12] Liu T, Lai J, Li Z and Li T 2025 Measurement-device-independent quantum-secret-sharing networks with linear Bell-state analysis *Phys. Rev. Appl.* **23** 034057
[13] Liu Q and Zhang M 2015 Generation and complete nondestructive analysis of hyperentanglement assisted by nitrogen-vacancy centers in resonators *Phys. Rev. A* **91** 062321
[14] Guo F-Q, Wu J-L, Zhu X-Y, Jin Z, Zeng Y, Zhang S, Yan L-L, Feng M and Su S-L 2020 Complete and nondestructive distinguishment of many-body Rydberg entanglement via robust geometric quantum operations *Phys. Rev. A* **102** 062410
[15] Deng F-G, Ren B-C and Li X-H 2017 Quantum hyperentanglement and its applications in quantum information processing *Sci. Bull.* **62** 46
[16] Walgate J, Short A J, Hardy L and Vedral V 2000 Local distinguishability of multipartite orthogonal quantum states *Phys. Rev. Lett.* **85** 4972
[17] Virmani S, Sacchi M F, Plenio M B and Markham D 2001 Optimal local discrimination of two multipartite pure states *Phys. Lett. A* **288** 62–68
[18] Hayashi M, Markham D, Murao M, Owari M and Virmani S 2006 Bounds on Multipartite entangled orthogonal state discrimination using local operations and classical communication *Phys. Rev. Lett.* **96** 040501
[19] Owari M and Hayashi M 2006 Local copying and local discrimination as a study for nonlocality of a set of states *Phys. Rev. A* **74** 032108
[20] Mattle K, Weinfurter H, Kwiat P G and Zeilinger A 1996 Dense coding in experimental quantum communication *Phys. Rev. Lett.* **76** 4656
[21] Cao C, Zhang L, Han Y-H, Yin P-P, Fan L, Duan Y-W and Zhang R 2020 Complete and faithful hyperentangled-Bell-state analysis of photon systems using a failure-heralded and fidelity-robust quantum gate *Opt. Express* **28** 2857
[22] Sheng Y-B, Deng F-G and Long G L 2010 Complete hyperentangled-Bell-state analysis for quantum communication *Phys. Rev. A* **82** 032318
[23] Kang Y-H, Chen Y-H, Shi Z-C, Huang B-H, Song J and Xia Y 2017 Complete Bell-state analysis for superconducting-quantum-interference-device qubits with a transitionless tracking algorithm *Phys. Rev. A* **96** 022304
[24] Ghosal P, Ghosal A, Das D and Maity A G 2023 Quantum superposition of causal structures as a universal resource for local implementation of nonlocal quantum operations *Phys. Rev. A* **107** 022613
[25] Walborn S P, Pádua S P and Monken C H 2003 Hyperentanglement-assisted Bell-state analysis *Phys. Rev. A* **68** 042313
[26] Li X-H and Ghose S 2017 Hyperentangled Bell-state analysis and hyperdense coding assisted by auxiliary entanglement *Phys. Rev. A* **96** 020303
[27] Schuck C, Huber G, Kurtsiefer C and Weinfurter H 2006 Complete deterministic linear optics Bell state analysis *Phys. Rev. Lett.* **96** 190501
[28] Olivo A and Grosshans F 2018 Ancilla-assisted linear optical Bell measurements and their optimality *Phys. Rev. A* **98** 042323
[29] Kong L-J *et al* 2019 Complete measurement and multiplexing of orbital angular momentum Bell states *Phys. Rev. A* **100** 023822
[30] Oreshkov O, Costa F and Brukner C 2012 Quantum correlations with no causal order *Nat. Commun.* **3** 1092
[31] Rubino G, Rozema L A, Feix A, Araújo M, Zeuner J M, Procopio L M, Brukner Č and Walther P 2017 Experimental verification of an indefinite causal order *Sci. Adv.* **3** e1602589
[32] Antesberger M, Quintino M T, Walther P and Rozema L A 2024 Higher-order process matrix tomography of a passively-stable quantum switch *PRX Quantum* **5** 010325
[33] Cao H *et al* 2023 Semi-device-independent certification of indefinite causal order in a photonic quantum switch *Optica* **10** 561
[34] Feix A, Araújo M and Brukner Č 2015 Quantum superposition of the order of parties as a communication resource *Phys. Rev. A* **92** 052326
[35] Chiribella G 2012 Perfect discrimination of no-signalling channels via quantum superposition of causal structures *Phys. Rev. A* **86** 040301
[36] Escandón-Monardes J, Delgado A and Walborn S P 2023 Practical computational advantage from the quantum switch on a generalized family of promise problems *Quantum* **7** 945
[37] Guérin P A, Feix A, Araújo M and Brukner Č 2016 Exponential communication complexity advantage from quantum superposition of the direction of communication *Phys. Rev. Lett.* **117** 100502
[38] Wei K *et al* 2019 Experimental quantum switching for exponentially superior quantum communication complexity *Phys. Rev. Lett.* **122** 120504
[39] Rubino G *et al* 2021 Experimental quantum communication enhancement by superposing trajectories *Phys. Rev. Res.* **3** 013093
[40] Yin P *et al* 2023 Experimental super-Heisenberg quantum metrology with indefinite gate order *Nat. Phys.* **19** 1122
[41] Agrawal G, Halder P and SenDe A 2025 Indefinite time directed quantum metrology *Quantum* **9** 1785
[42] Dieguez P R, Lisboa V F and Serra R M 2023 Thermal devices powered by generalized measurements with indefinite causal order *Phys. Rev. A* **107** 012423

[43] Xi C Liu X, Liu H, Huang K, Long X, Ebler D, Nie X, Dahlsten O and Lu D 2024 Experimental validation of enhanced information capacity by quantum switch in accordance with thermodynamic laws *Phys. Rev. Lett.* **133** 040401
[44] Liu W-Q, Meng Z, Song B-W, Li J, Wu Q-Y, Chen X-X, Hong J-Y, Zhang A-N and Yin Z-Q 2024 Experimentally demonstrating indefinite causal order algorithms to solve the generalized Deutsch's problem *Adv. Quantum Technol.* **7** 2400181
[45] Miguel-Ramiro J, Shi Z, Dellantonio L, Chan A, Muschik C A and Dür W 2023 Superposed quantum error mitigation *Phys. Rev. Lett.* **131** 230601
[46] Spencer-Wood H 2025 Indefinite causal key distribution *J. Phys. A* accepted (https://doi.org/10.1088/1751-8121/ae1e44)
[47] Liu W-Q and Wei H-R 2025 Deterministic generation of multiqubit entangled states among distant parties using indefinite causal order *Phys. Rev. Appl.* **23** 054075
[48] Zuo Z, Hanks M and Kim M S 2023 Coherent control of the causal order of entanglement distillation *Phys. Rev. A* **108** 062601
[49] Chiribella G, D'Ariano G M, Perinotti P and Valiron B 2013 Quantum computations without definite causal structure *Phys. Rev. A* **88** 022318
[50] Marletto C and Vedral V 2017 Gravitationally induced entanglement between two massive particles is sufficient evidence of quantum effects in gravity *Phys. Rev. Lett.* **119** 240402
[51] Zych M, Costa F, Pikovski I and Brukner Č 2019 Bell's theorem for temporal order *Nat. Commun.* **10** 3772